Acoustic Optimization of a Switched Reluctance Machine using Numerical Simulation

Benedikt Schmülling*, Knut Kasper**, and Kay Hameyer*
*Institute of Electrical Machines, RWTH Aachen University, Schinkelstr. 4, D-52056 Aachen, Germay
**Institute of Power Electronics and Electrical Drives, RWTH Aachen University, Jägerstr. 17/19, D-52066 Aachen, Germany
E-mail: Benedikt.Schmuelling@iem.rwth-aachen.de

***Abstract*— The excited audible noise of a switched reluctance machine (SRM) is a well known problem. Therefore, the acoustic optimization of SRMs is of high interest. A useful tool for the prediction of the acoustic behavior is the numerical simulation. In this paper the entire simulation path starting with the electromagnetic and structure-dynamic calculation up to the point of the acoustic simulation is introduced. Furthermore, simulation results of different optimization methods for an SRM are presented and discussed.**

***Index Terms*— FEM, BEM, Coupled Simulation, Acoustics, Audible Noise, Electrical Machines, SRM, Electromagnetic Energy Converters.**

I. Introduction

ACOUSTIC noise radiated from an SRM consists of three parts:

- The broad band fan and ventilation noise (500 - some kHz) results from air turbulences generated by the rotating motor.
- Friction of the bearings of the SRM is a further sound source, which generates single tones in the range larger than 3 kHz.
- Housing vibrations excited by the electromagnetic field of the SRM generate the magnetic noise, which consists of single tones in the entire range of audibility.

The presented calculation method discusses the noise radiation generated by electromagnetic forces.

In recent years switched reluctance machines have often been proposed as drives for cost-efficient applications. This can be based on the economical construction of the SRM and the price decline of power electronics. A disadvantage, which prevents the wide spread of the SRM, is its acoustic noise. Numerical simulations are one possibility to predetermine the acoustic behaviour of an SRM. Different variations of the machine design can be reviewed and compared before the expensive prototyping step. As an example, two different versions of an SRM are analyzed in this paper.

Switched reluctance machines consist of several mechanical and electrical parts. Fig. 1 shows the cross section of the active part of the presented SRMs.

The studied SRM versions differ in housing material and housing design (Fig. 2). Aluminum is the housing material of the first SRM studied. It is characterized by a low density compared to gray cast iron, which is the basic material of the second SRM housing studied. Furthermore, the two housing materials vary in Young's modulus. An advantage of aluminum is its lower weight. The cast iron SRM may radiate less noise than the aluminum SRM due to the higher density [1]. This potential benefit of the cast iron housing is analyzed in this paper.

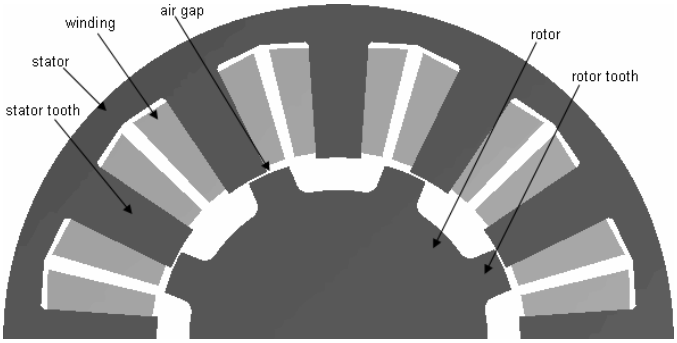

Fig. 1. Lamination of the studied SRM.

Another possibility to influence the audible noise of the SRM is the variation of the supplying current waveform. SRMs are able to reach a similar working point (i.e. nearly the same average torque at the same speed) by using different current intensities and different waveforms. The impact of four unequal currents on the audible noise of the SRM is discussed in this paper.

A numerical simulation of electrical machines is a coupled simulation that consists of three parts [2]:

1) The electromagnetic field computation to determine the electromagnetic forces acting on the stator,
2) the structure-dynamic simulation to calculate the resulting mechanical deformation (vibrations) of the SRM and
3) the acoustic simulation to estimate the radiated noise.

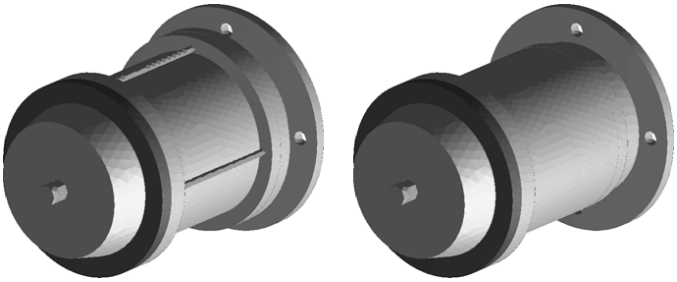

Fig. 2. SRM with aluminum (left) and cast iron (right) housing.

For this simulation chain a number of software programs have to be coupled. The main steps of this computation are described in the following chapters.

II. Preliminary Calculations

A. Electromagnetic Field Computation

The first step of the numerical simulation is the calculation of the electromagnetic field in the SRM. For this, the Finite-Element Method (FEM) is applied. The simulation is performed with a 2-dimensional model of the machine, which contains the electromagnetic active parts of the motor. Excitation parameters are the phase currents in the stator windings. Electromagnetic FEM computation is performed for steady-state operation.

The simulation of the motor is quasi-stationary for a defined number of angular increments. In every simulation step the rotor turns in dependance of speed n and time-step width Δt around an angle of $\Delta\alpha$. According to the rotor position, a new value for the current is assigned to the model. As a result of the time-discrete simulation the magnetic vector potential A is obtained.

Fig. 3 shows the vector potential distribution for one single time-step. Dark areas display a high and light-colored areas display a low value for A. The flux density distribution is computed by applying

$$\vec{B} = \operatorname{curl} \vec{A}. \tag{1}$$

The flux density distribution, presented in Fig. 4, shows that the highest values of B are found in the tooth tips of stator and rotor. From this flux density distribution other quantities can be derived. One is the torque T, another is the surface-force density σ. σ, which is required as excitation for the structure-dynamic model, is calculated for each time step using the Maxwell stress tensor method. Fig. 5 presents the resulting force excitation in a 2-dimensional model of the SRM. In the figure can be seen, that both the radial and the tangential forces are considered.

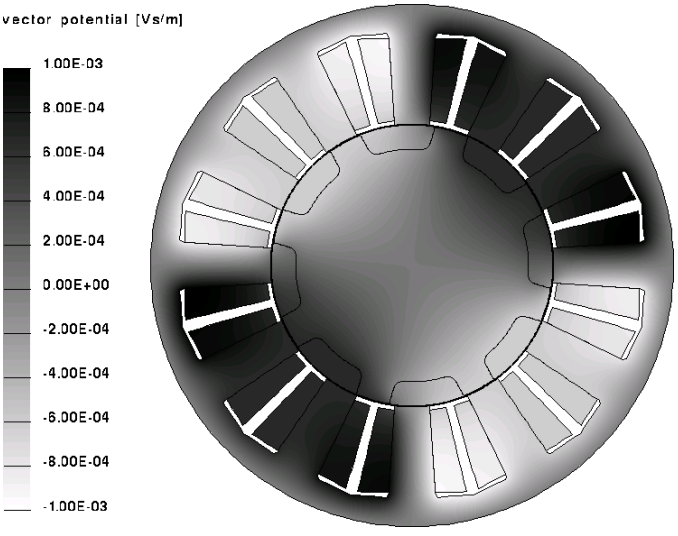

Fig. 3. Magnetic vector potential in the SRM for one single time step.

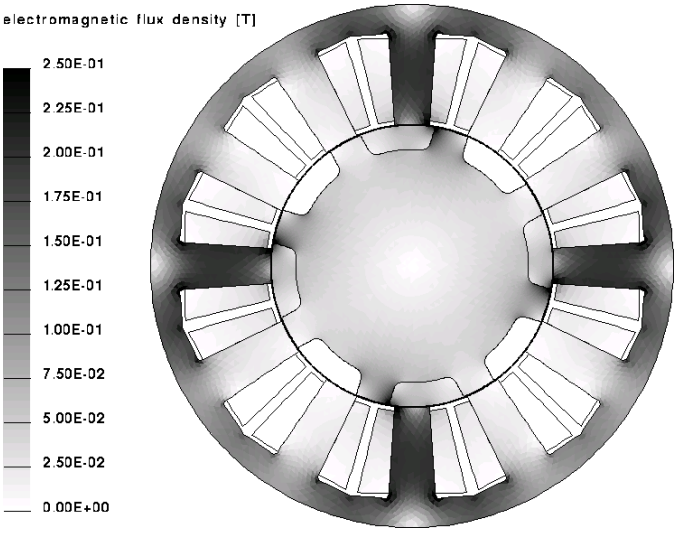

Fig. 4. Magnetic flux density in the SRM for one single time step.

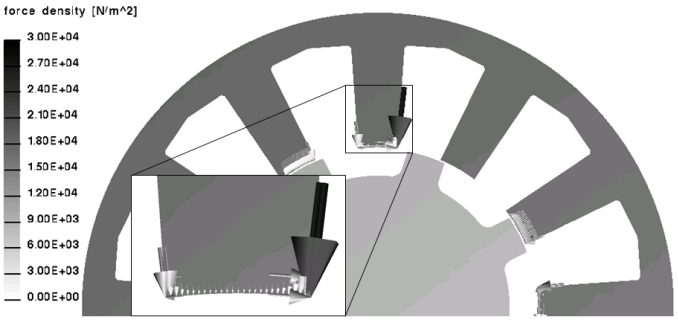

Fig. 5. Force density distribution in the SRM for one single time step.

Simulation of the electromagnetic surface-force density is also possible with a 3-dimensional simulation model. A benefit of a 3-dimensional FE-model is the possibility of considering geometry effects such as skewing. Nevertheless, 2-dimensional models are much smaller, so the computation time is not as long as for 3-dimensional models. A further advantage of 2-dimensional models is the higher accuracy due to the smaller FE-elements and the resulting higher discretization of the machine. Therefore, a 2-dimensional FE-model is applied in this paper.

B. Mechanical Deformation

The simulation of the mechanical deformation of the SRM also demands a numerical calculation. An analytical solution of the problem is not possible since number and complexity of the machine components are too high. Therefore, the FE-method is used. Numerous previous projects have proven the FE-method to be suitable for this application [3].

This simulation requires another model of the SRM. The mechanical model differs from the electromagnetic model since it has to consider all mechanical components of the machine. Housing, bearings, end shields, and further parts of the SRM have to be implemented to the model. The surrounding air is not included, since its damping influence on the expected small deformations is negligible. Fig. 6 shows

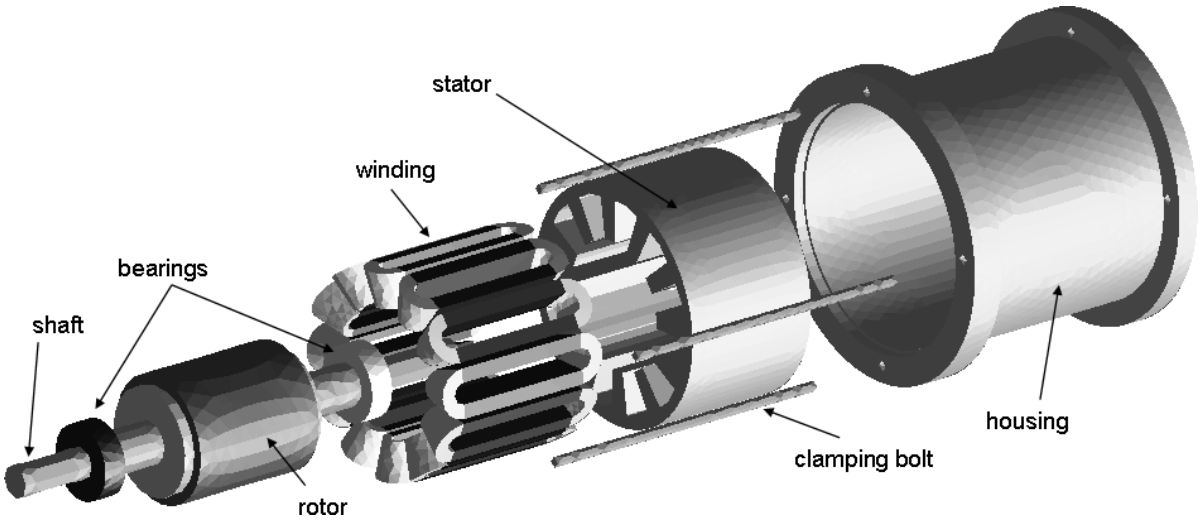

Fig. 6. Exploded view of the structure-dynamic model.

the mechanical model of the SRM. All mechanical contruction parts of the machine are included. The rotor of the SRM is modeled as a cylinder. Earlier structure-dynamic simulations of electrical machines (e.g. [3]) show, that the influence of the rotor on the housing deformation is marginal. Therefore, a detailed and complex replication of the rotor is not necessary. Aim of the structure dynamic calculation is the determination of the surface area velocity, which is the excitation value for the acoustic simulation. The deformation of the SRM is represented by the displacement of single nodes of the FE-model. The correlation between strain η and tension σ is given by

$$\sigma = \boldsymbol{H} \cdot \eta, \tag{2}$$

where H is Hooke's matrix. The entries of the matrix are defined by Young's modulus E and Poisson's ratio μ of the corresponding material. If the used materials are isotropic and homogenous, the Hooke's matrix H has the following form:

$$\boldsymbol{H} = \frac{E\cdot(1-\mu)}{(1-\mu)\cdot(1-2\mu)} \cdot \begin{pmatrix} 1 & a & a & 0 & 0 & 0 \\ a & 1 & a & 0 & 0 & 0 \\ a & a & 1 & 0 & 0 & 0 \\ 0 & 0 & 0 & b & 0 & 0 \\ 0 & 0 & 0 & 0 & b & 0 \\ 0 & 0 & 0 & 0 & 0 & b \end{pmatrix}, \tag{3}$$

with

$$a = \frac{\mu}{1-\mu} \quad \text{and} \quad b = \frac{1-2\mu}{2(1-\mu)}. \tag{4}$$

After dicretization of these equations [4] the oscillation equation results:

$$\boldsymbol{K} \cdot D + \boldsymbol{C} \cdot \dot{D} + \boldsymbol{M} \cdot \ddot{D} = F. \tag{5}$$

Here, K is the global stiffness matrix, D the vector of the node displacements, C the damping matrix, M the generalized mass matrix and F the excitation force. For the deployed harmonic analysis, with

$$\dot{D} = \frac{dD}{dt} = j\omega D \tag{6}$$

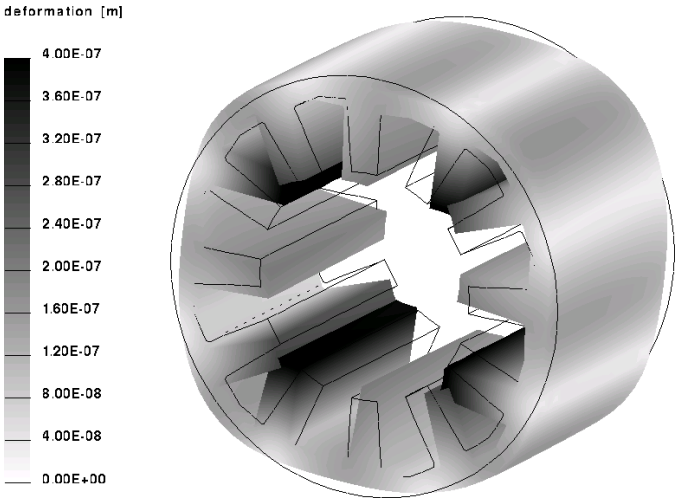

Fig. 7. Deformation of the stator at f = 3200 Hz.

follows

$$(\boldsymbol{K} + j\omega\boldsymbol{C} - \omega^2\boldsymbol{M}) \cdot D = F. \tag{7}$$

F is the complex surface-force density, which is determined by the electromagnetic simulation for all demanded frequencies. Fig. 7 shows the deformed stator of the SRM at $f = 3200\,\mathrm{Hz}$ as a result of the mechanical simulation.

The node displacement D is used as input value of the acoustic simulation. In special cases it could be an advantage to evaluate the periodic deformation of an electrical machine instead of the acoustic behaviour. In such cases the body-sound level can be determined at fixed locations. The body-sound level is an admeasurement for the vibrations of a local point of the analyzed machine. Alternatively, the body-sound index can be established, which represents an integral quantity for the entire machine. Using these two values, it is possible to compare the deformation behaviour of different excitations.

A more detailed description of the structure-dynamic simulation can be found in [4].

III. Acoustic Simulation

As excitation for the acoustic simulation the mechanical deformation of the machine is converted to the velocity $\vec{v}$ of each surface node of the mechanical model. In principle, calculation of acoustic fields is also possible with the FEM. However, for calculation of air-borne noise this method is unfavourable since the entire calculation area has to be discretized. An alternative is offered by the Boundary-Element Method (BEM) [5]. The BEM is based on integral equations of the problem. These integral equations apply to the boundary layer of the calculation area. Precondition for using the BEM is a linear and homogeneous medium. This requirement is fulfilled by air.

After using a 2-dimensional FE-model for the simulation of the electromagnetic force excitation and using a 3-dimensional FE-model for the calculation of the structure-dynamic behaviour, the acoustic simulation employing the BEM requires a third machine model. This model only consists of the outer surface mesh of the device, which represents the noise radiating area of the motor. The mechanical velocity $\vec{v}$ is transferred to this acoustic mesh. The main equation in the acoustic problem is the Helmholtz differential equation

$$\Delta \underline{p} + k^2 \cdot \underline{p} = 0 \tag{8}$$

with the sound pressure p and wave number $k = \frac{\omega}{c}$. Here, ω is the angular frequency and c the sound velocity. For solving this differential equation, two conditions must be fulfilled. First, the surface of the sound radiating body has to be smooth. Second, the normal vector of the surface area must point outwards. For the numerical solving of the problem, the method of the weighted residual

$$\int_{\Omega} (\Delta \underline{p} + k^2 \cdot \underline{p}) u^* \, d\Omega = 0 \tag{9}$$

with a weighting function u^* is used. After further calculations [6] the following equation system results:

$$\boldsymbol{H} \cdot \underline{p} = \boldsymbol{G} \cdot \vec{v}. \tag{10}$$

H and G are system matrices and the velocity vector $\vec{v}$ is the excitation value. The sound pressure p is determined by numerical evaluation of (10). After simulation no result is available for the surrounding air, since there is no discretization. Therefore, the acoustic attributes are evaluated on predetermined points or surfaces. On the one hand the distribution of sound pressure can be analyzed graphically. This is used to identify the location of maximum noise radiation.

Fig. 8 represents the sound pressure on a hemispherical evaluation area around the acoustic SRM model for a discrete frequency of $f = 4400\,\mathrm{Hz}$. A dark area in the figure means a higher pressure on that position on the evaluation surface.

On the other hand the sound particle velocity vector (Fig. 9) can be used to evaluate the direction of the radiated noise. Here, the same hemispherical area is used as for the evaluation of the sound pressure. Each vector in the figure represents the sound particle velocity on the respective area element. In both figures (8 and 9) can be seen, that the main part of the noise radiation is in axial direction for $f = 4400\,\mathrm{Hz}$ at the

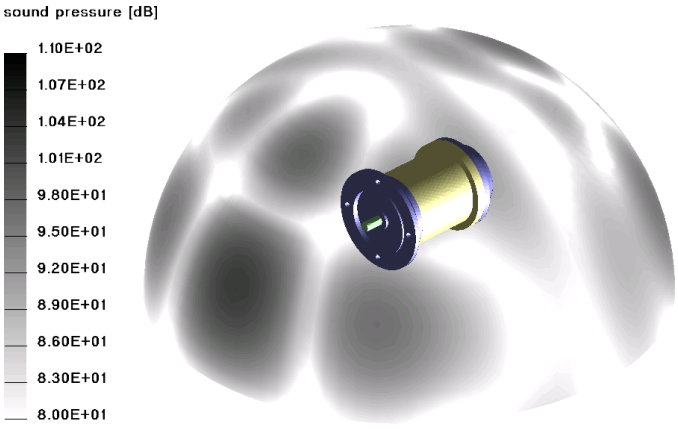

Fig. 8. Sound pressure distribution on the analysis sphere at f = 4400 Hz.

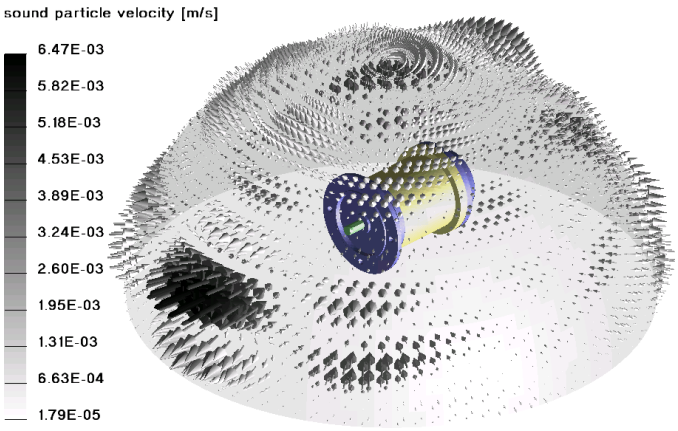

Fig. 9. Sound particle velocity field on the analysis sphere at f = 4400 Hz.

simulated point of operation. These graphical representations allow qualitative statements for comparing different machine constructions. However, for the quantification of design modifications an integral value is more interesting.

For this, the acoustic power P is determined:

$$P = \oint_{\partial\Gamma} \vec{I} \cdot \, d\partial\vec{\Gamma}. \tag{11}$$

An enveloping surface $\partial\Gamma$ is allocated arround an air volume Γ, which yields the noise radiating body. The normal component of the sound intensity $\vec{I}$ is integrated over the enveloping surface. Sound intensity is defined as follows:

$$\vec{I} = \frac{1}{2} Re\{\underline{p} \cdot \underline{\vec{v}}^*\}. \tag{12}$$

Sound particle velocity $\underline{\vec{v}}$ and sound pressure $\underline{p}$ are the simulated values. The acoustic power P describes the power output of the sound source. All emitted energy passes through an enveloping surface around the machine. Here, the bottom of the hemispherical surface is reverberant, so all the noise is radiated through the evaluation area.

The level quantity L_P is introduced since the value of the acoustic power alternates over multiple decades. L_P is a logarithmic value of the acoustic power, recalculated from

unit W to unit dB:

$$L_P = 10 \cdot \log_{10} \frac{P}{P_0}. \tag{13}$$

P_0 is a reference variable for the acoustic power and amounts to $P_0 = 10^{-12}$ W. The acoustic power level L_P is an adequate quantitative value for the analysis of the effectiveness of design modifications for the acoustic optimization since it is an explicit value for the comparison of different optimization methods.

IV. Results

The presented simulation is performed for different variations of the SRM. As described in the preceding sections, the aim of these variations is the analysis of a possible acoustic improvement without prototyping.

A. Waveform Optimization

The idea in this study to lower the excited audible noise of an SRM is a modification of the current waveform. Fig. 10 represents four different 3-phase currents, which differ in maximum value, operating interval, and switching angles. Current 1 describes a standard waveform for SRMs. The other waveforms show modified currents, which are generated in consideration of different optimization strategies [7]. The aim of all procedures is the reduction of the radial forces for all critical frequencies, which are the main reason of the housing vibrations. To compare the noise produced by different current waveforms the point of operation of the machine should be the same, i.e. the average torque and the speed of the SRM have to be the same for all waveforms studied. As working point for the simulation presented in this paper an average torque of $T = 3.1\,\mathrm{Nm}$ is used. The rotational speed of the SRM is $n = 3000\,\mathrm{rpm}$. All current waveforms presented in Fig. 10 satisfy these preconditions.

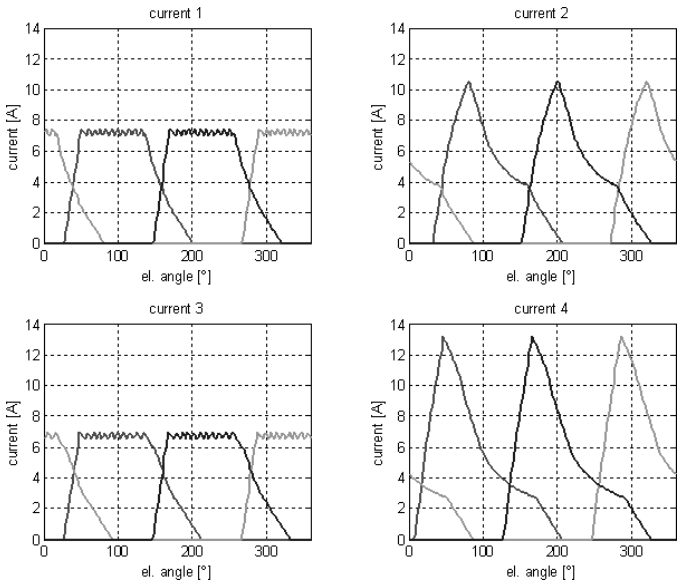

Fig. 10. Four different current waveforms used for the analysis of the SRM.

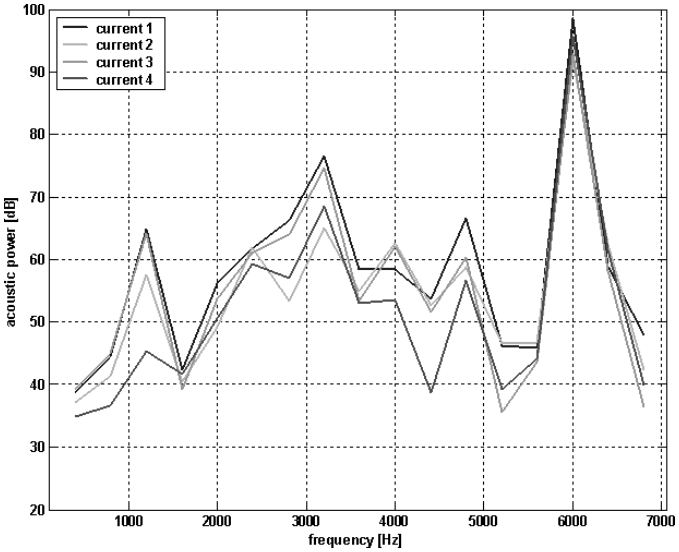

Fig. 11. Acoustic power of the SRM with an aluminum housing at $n = 3000\,\mathrm{rpm}$.

Fig. 11 shows the acoustic power level L_P of the SRM at $n = 3000\,\mathrm{rpm}$ in a frequency range from 0 Hz to 7000 Hz. The figure presents the simulation results of the four different currents shown in Fig. 10. When comparing the four currents, wide differences in the acoustic behaviour can be seen. For some discrete frequencies the deviation of the values is clear-cut. At $f = 1200\,\mathrm{Hz}$, $f = 4000\,\mathrm{Hz}$, and $f = 4400\,\mathrm{Hz}$ current 4 radiates the lowest acoustic power by far. Other discrete frequencies show less or no major differences. $f = 6000\,\mathrm{Hz}$ is a resonant frequency in the bearing brackets, which declares the high acoustic power values at this frequency. Nevertheless, by imposing different waveforms of the supplying currents it is possible to influence the acoustic behaviour of SRMs.

B. Alternative Housing Materials

Another strategy for the acoustic optimization of the SRM is the use of different housing materials. Substances with a different density and a different Young's modulus tend to different deformations [1], [8]. Thus, the radiation of audible noise is also influenced. In this paper an SRM with an aluminum housing is compared to an SRM with a housing made of gray cast iron. The material densities of cast iron ρ_c and aluminum ρ_a have the following values:

$$\rho_c = 7200\,\frac{\mathrm{kg}}{\mathrm{m}^2} \tag{14}$$

and

$$\rho_a = 2700\,\frac{\mathrm{kg}}{\mathrm{m}^2}. \tag{15}$$

So, the density of cast iron is much higher than the density of aluminum. The values of the Young's moduli of both materials E_c and E_a amount to

$$E_c = 9.5 \cdot 10^4\,\frac{\mathrm{N}}{\mathrm{mm}^2} \tag{16}$$

and

$$E_a = 7.2 \cdot 10^4\,\frac{\mathrm{N}}{\mathrm{mm}^2}. \tag{17}$$

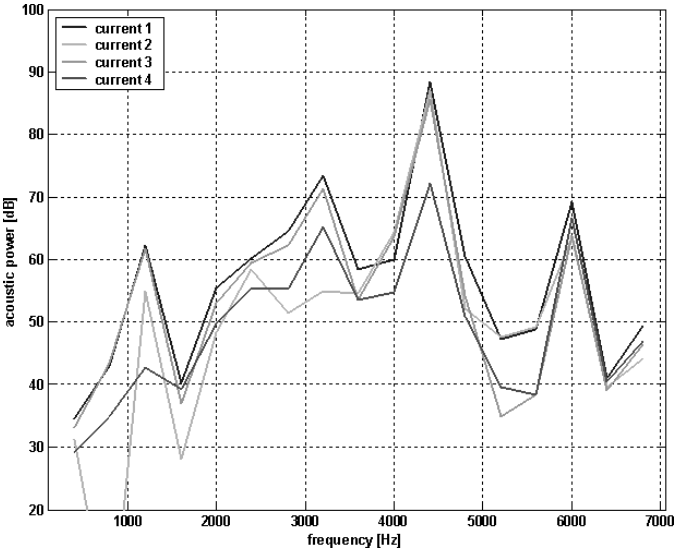

Fig. 12. Acoustic power of the SRM with a gray cast iron housing at $n = 3000\,\mathrm{rpm}$.

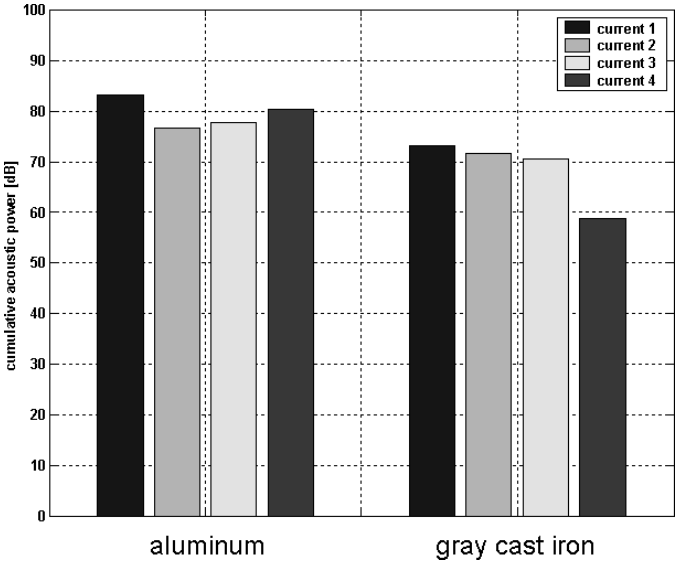

Fig. 13. Cumulative acoustic power of the SRM.

Here, the value of the cast iron is also higher than the aluminum value. Fig. 11 shows the acoustic power of the SRM with an aluminum housing, Fig. 12 presents the acoustic power of the SRM with a cast iron housing for the same working point in the same frequency range.

The acoustic power for discrete frequencies in the first diagram is distinct from the acoustic power shown in the second one. The average level of the power for all four currents is about $L_P = 70\,\mathrm{dB}$ for the aluminum housing at the frequency of $f = 3200\,\mathrm{Hz}$, for example. An SRM with cast iron housing only radiates noise with an acoustic power level of about $L_P = 65\,\mathrm{dB}$. For other frequencies (for example at $f = 4400\,\mathrm{Hz}$) the differences are reversed and the cast iron housing radiates more audible noise. Therefore, the results require a further evaluation to identify the best SRM variation.

C. Synopsis

To estimate the optimum variation of the SRM it is necessary to calculate cumulative acoustic power for all housing materials and all currents. The cumulative acoustic power level L_{Pcum} is the average of all acoustic powers in the range of audible frequencies. Since the values are given in unit dB they have to be recalculated to unit W. In Fig. 13 the cumulative acoustic power level for all presented variations of the SRM is shown. In the diagram it can be seen, that the acoustic power radiated by the SRM with a cast iron housing always is below the acoustic power radiated by the aluminum housing. Furthermore, current 4 in combination with the cast iron housing produces the fewest audible noise by far. All presented results show a good accordance to air-borne sound measurements.

V. Conclusion

Numerical simulations of the audible noise of an SRM consist of several coupled computation steps. The main parts of the entire simulation are described in this paper. With respect to its acoustic behaviour every type of electromagnetic energy converter can be analyzed and evaluated by the presented simulation approaches. Furthermore, the paper presents the high optimization potential concerning audible noise of the analyzed application. The influence of current waveform variations on the radiated sound of the SRM is demonstrated. A further section of this paper presents the simulation results for the use of different housing materials. In a synopsis the optimum combination of both optimization methods is established. By regarding these computation results, necessary adjustments for lowering the motor noise can be done before prototyping.

References

[1] T. J. E. Miller, *Switched Reluctance Motors and Their Control*. Oxford: Magna Physics Publishing and Clarendon Press, 1993.

[2] M. Furlan, A. Cernigoj, and M. Boltezar, “A coupled electromagnetic-mechanical-acoustic model of a DC electric motor,” *COMPEL: The International Journal for Computation and Mathematics in Electrical and Electronic Engineering*, vol. 22, no. 4, 2003.

[3] C. Schlensok, D. van Riesen, T. Küest, and G. Henneberger, “Acoustic simulation of an induction machine with squirrel-cage rotor,” *COMPEL: The International Journal for Computation and Mathematics in Electrical and Electronic Engineering*, vol. 25, no. 2, 2006.

[4] I. Ramesohl, S. Küppers, W. Hadrys, and G. Henneberger, “Three Dimensional Calculation of Magnetic Forces and Displacements of a Claw-Pole Generator,” *IEEE Transactions on Magnetics*, vol. 32, no. 3, pp. 1685–1688, May 1996.

[5] F. Hartmann, *Introduction to boundary elements method*. Berlin: Springer-Verlag, 1989.

[6] T. Bauer and G. Henneberger, “Three Dimensional Calculation and Optimization of the acoustic Field of an induction Furnace caused by electromagnetic Forces,” *IEEE Transactions on Magnetics*, vol. 35, no. 3, pp. 1598–1601, May 1999.

[7] J. O. Fiedler and R. W. De Doncker, “Extended Analytic Approach to Acoustic Noise in Switched Reluctance Drives,” *PESC 02. 2002 IEEE 33rd Annual*, vol. 4, pp. 1960–1964, June 2002.

[8] Z. Tang, P. Pillay, A. Omekanda, C. Li, and C. Cetinkaya, “Measurement of Young’s modulus for switched reluctance motor vibration determination,” *IEEE International Electric Machines and Drives Conference*, vol. 3, pp. 1590–1595, 2003.